J. Membrane Biol. 143, 103–113 (1995)

The Journal of
Membrane
Biology

Kinetics and Specificity of the Renal Na^+/*myo*-Inositol Cotransporter Expressed in *Xenopus* Oocytes

K. Hager*,†, A. Hazama,†, H.M. Kwon[2], D.D.F. Loo[1], J.S. Handler[2], E.M. Wright[1]**

[1]Department of Physiology, UCLA School of Medicine, Center for the Health Sciences, 10833 Le Conte Avenue, Los Angeles, California 90024-1751

[2]Division of Nephrology, Department of Medicine, Johns Hopkins University School of Medicine, Baltimore, Maryland 21205-2196

Received: 29 July 1994/Revised: 10 October 1994

Abstract. The two-microelectrode voltage clamp technique was used to examine the kinetics and substrate specificity of the cloned renal Na^+/*myo*-inositol cotransporter (SMIT) expressed in *Xenopus* oocytes. The steady-state *myo*-inositol-induced current was measured as a function of the applied membrane potential (V_m), the external *myo*-inositol concentration and the external Na^+ concentration, yielding the kinetic parameters: $K_{0.5}^{MI}$, $K_{0.5}^{Na}$, and the Hill coefficient n. At 100 mM NaCl, $K_{0.5}^{MI}$ was about 50 μM and was independent of V_m. At 0.5 mM *myo*-inositol, $K_{0.5}^{Na}$ ranged from 76 mM at $V_m = -50$ mV to 40 mM at $V_m = -150$ mV. n was voltage independent with a value of 1.9 ± 0.2, suggesting that two Na^+ ions are transported per molecule of *myo*-inositol. Phlorizin was an inhibitor with a voltage-dependent apparent K_I of 64 μM at $V_m = -50$ mV and 130 μM at $V_m = -150$ mV. To examine sugar specificity, sugar-induced steady-state currents (at $V_m = -150$ mV) were recorded for a series of sugars, each at an external concentration of 50 mM. The substrate selectivity series was *myo*-inositol, *scyllo*-inositol > L-fucose > L-xylose > L-glucose, D-glucose, α-methyl-D-glucopyranoside > D-galactose, D-fucose, 3-*O*-methyl-D-glucose, 2-deoxy-D-glucose > D-xylose. For comparison, oocytes were injected with cRNA for the rabbit intestinal Na^+/glucose cotransporter (SGLT1) and sugar-induced steady-state currents (at $V_m = -150$ mV) were measured. For oocytes expressing SGLT1, the sugar selectivity was: D-glucose, α-methyl-D-glucopyranoside, D-galactose, D-fucose, 3-*O*-methyl-D-glucose > D-xylose, L-xylose, 2-deoxy-D-glucose > *myo*-inositol, L-glucose, L-fucose. The ability of SMIT to transport glucose and SGLT1 to transport *myo*-inositol was independently confirmed by monitoring the Na^+-dependent uptake of ^{3}H-D-glucose and ^{3}H-*myo*-inositol, respectively. In common with SGLT1, SMIT gave a relaxation current in the presence of 100 mM Na^+ that was abolished by phlorizin (0.5 mM). This transient current decayed with a voltage-sensitive time constant between 10 and 14 msec. The presteady-state current is apparently due to the reorientation of the cotransporter protein in the membrane in response to a change in V_m. The kinetics of SMIT is accounted for by an ordered six-state nonrapid equilibrium model.

Key words: Na^+/*myo*-inositol cotransport — Na^+/glucose cotransport — Kinetics — Electrophysiology — *Xenopus* oocytes

Introduction

Myo-inositol is an important precursor in the biosynthesis of inositol phosphates and phospholipids that play a central role in membrane and cell signaling. Furthermore, *myo*-inositol is accumulated in many cells in the body, especially the retina and renal medulla, and serves as a nonperturbing osmolyte in cells under osmotic stress (*see* Garcia-Perez & Burg, 1991). Apart from osmoregulation, there is interest in the role of the *myo*-inositol transporter in such diverse topics as delivery of *myo*-inositol to the brain across the blood-brain barrier, and development of complications in diabetes mellitus (*see* Yorek et al., 1991; Yorek, Stefani & Moore, 1991).

Intracellular accumulation of *myo*-inositol occurs by a Na^+-dependent, phlorizin-sensitive mechanism. The

* *Present address:* W.M. Keck Biotechnology Resource Laboratory, Boyer Center for Molecular Medicine, Rm. 305A, Yale University, 295 Congress Ave., New Haven, Connecticut 06536-0812

** *Present address:* National Institute for Physiological Sciences, Department of Cell Physiology, Okazaka, 444, Japan

† Contributed equally to this work

Correspondence to: D.D.F. Loo

Table 1. Glucose and *Myo*-inositol contamination of sugar substrates

Sugar	Glucose	*myo*-Inositol
L-Fucose	<0.002%	<0.002%
D-Fucose	0.28%	<0.001%
D-Xylose	ND[a]	<0.002%
myo-Inositol	<0.025%	
αMDG	<0.2%	ND[a]

All values given for contamination are in mole percent of the sugar listed.
[a] Not determined because of very similar retention times for the two sugars.

myo-inositol transporter (SMIT) has recently been cloned, sequenced and expressed in *Xenopus* oocytes (Kwon et al., 1992), and is a member of the Na^+/glucose cotransporter family. There is 49% identity between SMIT and SGLT1, and this raises questions about similarities in transport mechanisms and substrate specificity. In this study we have used electrophysiological and tracer methods to examine both the kinetics and specificity of SMIT expressed in *Xenopus* oocytes and to compare the results with those obtained for SGLT1. We show that both SMIT and SGLT1 share the same transport mechanism and have overlapping substrate specificity. This provides important clues about the depletion of intracellular *myo*-inositol in diabetes mellitus.

Materials and Methods

Chemicals

All sugar substrates were purchased from Sigma Chemical (St. Louis, MO). Phlorizin was from Fluka (Ronkonkoma, NY). Other chemicals were reagent grade and obtained from either Sigma or Baker (Phillipsburg, NJ). The purity of the various sugars (Table 1) was assessed by high pressure liquid chromatography on a Carbopak PA1 column (Dionex) with pulsed amperometric detection (LaCourse, Mead & Johnson, 1990; Mopper et al., 1991).

In Vitro Transcription and Oocyte Assays

pSMIT, which contains the cDNA for the canine kidney Na^+/*myo*-inositol cotransporter (Kwon et al., 1992), was linearized by digestion with Not I and the resulting template transcribed by T7 RNA polymerase to give capped cRNA using either the method of Krieg and Melton (1984) or more recently a MEGAscriptTM transcription kit (Ambion, Austin, TX). Similarly, pMJC424, a plasmid containing the cDNA for the rabbit intestinal Na^+/glucose cotransporter (Hediger et al., 1987), was linearized by digestion with Xba I and the resulting template transcribed by T3 RNA polymerase. cRNA was diluted with H_2O to a concentration of 0.5 μg/μl and 50 nl was injected into each *Xenopus* oocyte. Oocytes were obtained from laboratory-raised adult female *Xenopus laevis* (Nasco, Fort Atkinson, WI). One day prior to injection, oocytes were dissected from pieces of the ovary and incubated with collagenase to remove the follicular cell layer (Colman, 1984). After three days of incubation in Barth's solution (concentrations in mM: 88 NaCl, 1 KCl, 0.33 $Ca(NO_3)_2$, 0.41 $CaCl_2$, 0.82 $MgSO_4$, 2.4 $NaHCO_3$, 10 HEPES, pH 7.4) plus 100 μg/ml gentamycin sulfate, the injected oocytes were assayed for transport activity. Na^+-dependent glucose transport into oocytes was measured as previously described (Ikeda et al., 1989), except that the radioactive substrate was D-[6-^{3}H]-glucose (36 Ci/mmol; New England Nuclear), the total glucose concentration was 10 μM, and the oocytes were incubated with the radioactive substrate for 30 min at 22°C. Na^+-dependent uptake of *myo*-[^{3}H]-Inositol (80 Ci/mmol; Amersham) into oocytes was determined in the same manner (10 μM total *myo*-inositol concentration), except that the oocytes were incubated with the radioactive substrate for 20 min at 22°C. Electrophysiological studies of injected oocytes were performed ≥6 days following cRNA injection.

Electrophysiological Methods

The membrane potential of cRNA-injected oocytes was controlled using the two-microelectrode voltage clamp technique (Birnir, Loo & Wright, 1991; Parent et al., 1992*a*; Loo et al., 1993). The command voltage was applied by an IBM-compatible computer running pCLAMP software (Axon instruments, Foster City, CA). Current signals were filtered at 5 kHz using an 8-pole Bessel filter (Model 902, Frequency Devices, Haverhill, MA) and sampled at 50 μsec. The resistance of the microelectrodes used to record voltage and inject current ranged from 1–2 and 0.5–1 MΩ, respectively. The temperature of the oocyte bath solution was maintained at 25°C by a Peltier effect device. In most experiments the membrane potential was held at $V_{hold} = -50$ mV. To obtain a current-voltage (*I-V*) relationship, the membrane potential was rapidly stepped from the holding potential to a series of values generally between −10 and −150 mV, each differing by 20 mV. The pulse duration was 100 msec, and between pulses there was a 1 sec interpulse interval at the holding potential. To reduce noise, currents from 10 runs were averaged. The oocyte was continuously perfused in a Na solution containing (in mM): 100 NaCl, 1 KCl, 1 $CaCl_2$, 1 $MgCl_2$, 10 HEPES-Tris, pH 7.4. For the measurement of substrate-induced current, each substrate was added to the perfusing Na^+ solution. To examine the Na^+ dependence of the *myo*-inositol-induced current, NaCl in the Na^+ solution was replaced iso-osmotically by cholineCl.

Results

Myo-Inositol-induced Current in SMIT cRNA-injected Oocytes

Figure 1*A* shows the current records from a SMIT cRNA-injected oocyte before application of *myo*-inositol. The membrane potential was stepped from the holding potential ($V_{hold} = -50$ mV) to a value between −10 and −150 mV in 20 mV increments. At $t \leq 50$ msec, relaxation currents were clearly observed and will be described in a later section. Upon the addition of 1 mM *myo*-inositol to the bath solution, the inward steady-state current (measured at 100 msec) increased concomitant with a large reduction of the presteady-state current (Fig. 1*B*). The steady-state current-voltage (*I-V*) relationships for the SMIT cRNA-injected oocyte measured in the absence and presence of 1 mM *myo*-inositol (Fig. 1*A* and

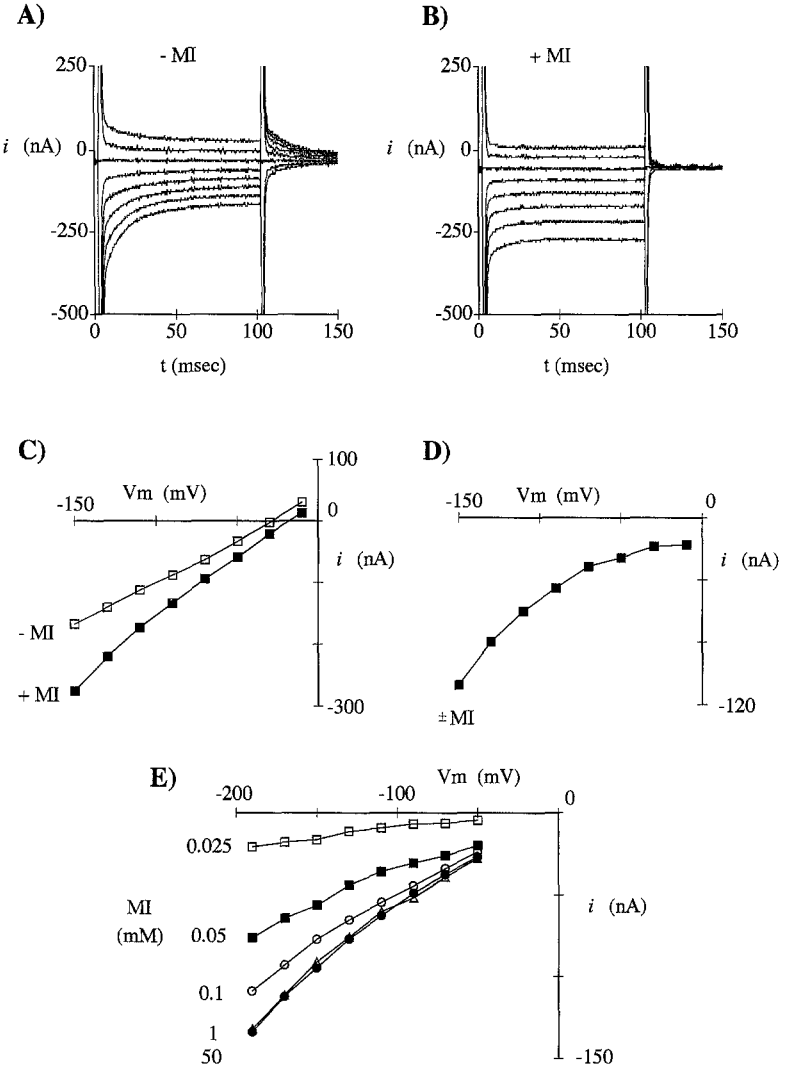

Fig. 1. *Myo*-inositol-induced current in a SMIT cRNA-injected oocyte. The current was recorded from an injected oocyte in the absence (*A*) and presence (*B*) of 1 mM *myo*-inositol (*MI*). Steady-state current measured with or without incubation of the oocyte in 1 mM *myo*-inositol is plotted as a function of the membrane potential (*C*). Subtraction of the two *I-V* curves in *C* gives the *I-V* relationship of the *myo*-inositol-induced steady-state current (*D*). The *myo*-inositol-induced steady-state current is plotted as a function of voltage at different *myo*-inositol concentrations (*E*).

B) are depicted in Fig. 1*C*. The difference between the two sets of data in Fig. 1*C* yielded the *I-V* curve for the *myo*-inositol-induced steady-state current (Fig. 1*D*). Note that the current increased with hyperpolarization and did not saturate within the voltage range of −10 to −150 mV, a result which is similar to the GABA-induced steady-state current of the Na^+/Cl^-/GABA cotransporter (Mager et al., 1993). In contrast, the α-methyl-D-glucopyranoside (αMDG)-induced current of SGLT1 saturated between −10 and −150 mV (*see* Fig. 4*B* and Parent et al., 1992*a*).

Voltage Dependence of I_{max}^{MI} and $K_{0.5}^{MI}$

To examine the influence of membrane voltage on the kinetic parameters, the *myo*-inositol-induced steady-state current was measured as a function of the extracellular *myo*-inositol concentration. The *myo*-inositol-induced current increased with increasing external *myo*-inositol concentration and saturated at 1 mM (Fig. 1*E*). The average of *myo*-inositol-induced steady-state currents, recorded from three SMIT cRNA-injected oocytes, was fitted to Eq. (1):

$$I = I_{max}^{MI}\,[MI]/(K_{0.5}^{MI} + [MI]), \quad (1)$$

yielding the kinetic parameters, $K_{0.5}^{MI}$ and I_{max}^{MI} as a function of voltage. I_{max}^{MI} is the maximum current at saturating external *myo*-inositol concentration [MI], and $K_{0.5}^{MI}$ is the concentration of *myo*-inositol where the current is one-half of the maximum. Within the membrane potential range of −50 to −150 mV, $K_{0.5}^{MI}$ was 55 μM (53 ± 6 μM at −150 mV; and 57 ± 8 μM at −50 mV). This value of $K_{0.5}^{MI}$ is close to the value of 31–33 μM reported for transport assays performed on both MDCK cells and SMIT cRNA-injected oocytes (Kwon et al., 1992). I_{max}^{MI} increased as the membrane potential increased from −50 to −150 mV but did not saturate (*see* Fig. 1*D*).

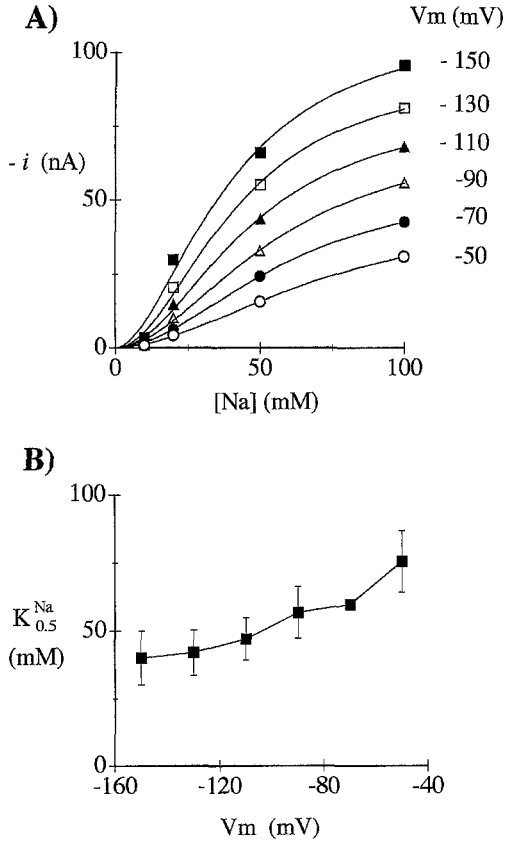

Fig. 2. Dependence of the *myo*-inositol-induced steady-state current on the concentration of external Na. The steady-state current induced by 0.5 mM *myo*-inositol was measured for a SMIT cRNA-injected oocyte as a function of membrane potential and external Na concentration (*A*). The $K_{0.5}^{Na}$ was derived by fitting the data to the Hill equation:

$$I = I_{max} [Na]^n/((K_{0.5}^{Na})^n + [Na]^n), \quad (4)$$

and is plotted as a function of membrane potential in *B*. The errors are standard errors of the fit.

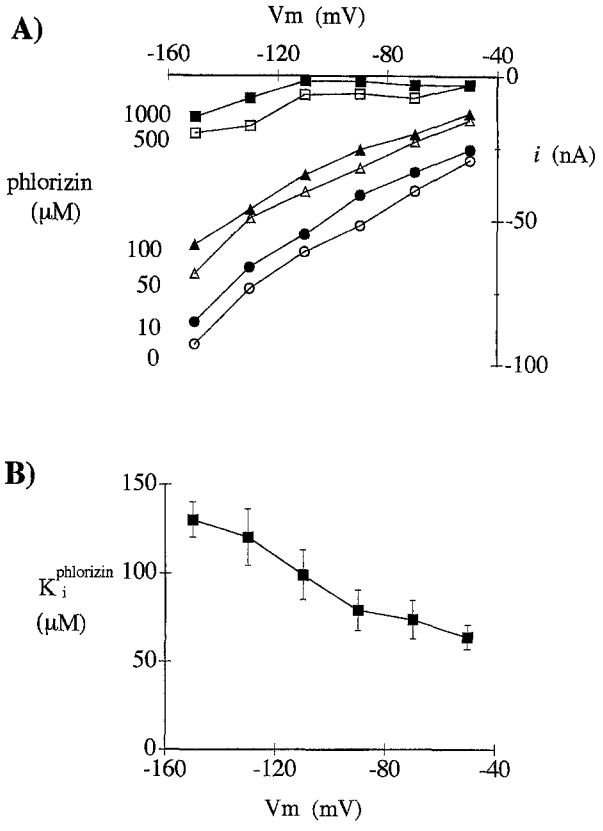

Fig. 3. Inhibition of the *myo*-inositol-induced steady-state current by external phlorizin. The *I-V* relationship for the *myo*-inositol-induced steady-state current at several phlorizin concentrations was recorded for a SMIT cRNA-injected oocyte (*A*). Bath solution contained 50 μM *myo*-inositol. The data were fit to a competitive inhibition model using nonlinear regression yielding $K_I^{phlorizin}$ as a function of membrane potential (*B*).

Voltage Dependence of I_{max}^{Na} and $K_{0.5}^{Na}$

Figure 2*A* shows the steady-state current induced by 0.5 mM *myo*-inositol as a function of extracellular Na. With the substitution of external Na^+ by choline, the *myo*-inositol-induced current decreased and totally disappeared at $[Na]_o$ = 0 mM. The plot of the *myo*-inositol-induced current as a function of external Na concentration was sigmoidal and the data were fit to Eq. (2):

$$I = I_{max}^{Na} [Na]^n/((K_{0.5}^{Na})^n + [Na]^n), \quad (2)$$

where I_{max}^{Na} is the maximum current at saturating external Na concentration, $K_{0.5}^{Na}$ is the concentration of Na^+ where the current is one-half of the maximum, and n is the Hill coefficient for Na^+. Figure 2*B* presents the voltage dependence of $K_{0.5}^{Na}$. $K_{0.5}^{Na}$ increased slightly with depolarization of the membrane (40 ± 10 mM at −150 mV; 76 ± 11 mM at −50 mV). A value of approximately 2 was obtained for the Hill coefficient (n), suggesting that two Na^+ ions are transported per molecule of *myo*-inositol. The Hill coefficient did not vary appreciably with membrane voltage (*data not shown*). I_{max}^{Na} increased with hyperpolarization of the membrane and did not saturate within the voltage range tested (−50 to −150 mV, *data not shown*).

Phlorizin Inhibition of *myo*-Inositol-Induced Steady-State Current

Phlorizin is a competitive inhibitor of SGLT1 (Ikeda et al., 1989) and is reported to inhibit SMIT (Kwon et al., 1992). To measure the inhibition constant for phlorizin ($K_I^{phlorizin}$) a SMIT cRNA-injected oocyte was incubated with 50 μM *myo*-inositol and the *myo*-inositol-induced steady-state current was recorded as a function of membrane voltage in the presence of different external concentrations of phlorizin. Figure 3*A* presents *I-V* curves

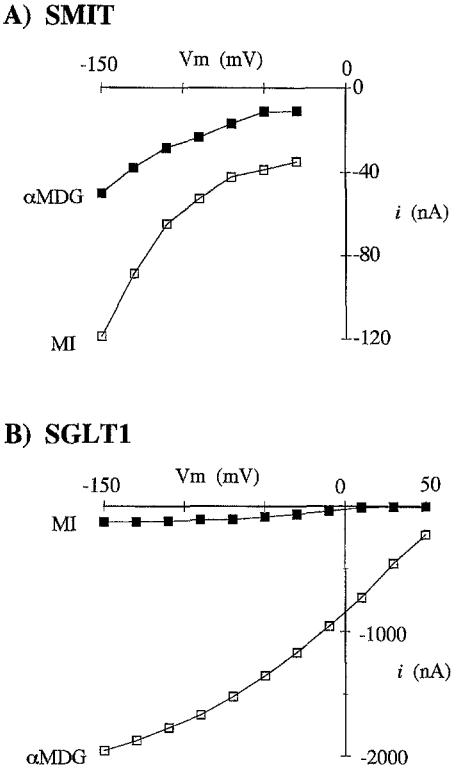

Fig. 4. *Myo*-inositol and αMDG-induced steady-state currents in SMIT and SGLT1 cRNA-injected oocytes. Steady-state current induced by *myo*-inositol and αMDG as a function of membrane potential is plotted for a SMIT cRNA-injected oocyte (*A*) and a SGLT1 cRNA-injected oocyte (*B*). External *myo*-inositol and αMDG concentrations were 50 mM.

measured at different extracellular phlorizin concentrations. Increasing the concentration of phlorizin decreased the *myo*-inositol-induced steady-state current. Nonlinear regression of the data to a competitive inhibition model provided estimates of the apparent K_I and its dependence on voltage (Fig. 3*B*). The phlorizin K_I was voltage dependent and ranged from 64 ± 7 μM at −50 mV to 130 ± 10 μM at −150 mV, values which are at least fivefold higher than the voltage-independent phlorizin K_I of 6–10 μM reported for SGLT1 (Ikeda et al., 1989; Birnir et al., 1991).

Sugar Specificity

Since SMIT and SGLT1 share 49% amino acid sequence identity, it proved interesting to measure their ability to transport both *myo*-inositol and αMDG. Either 50 mM *myo*-inositol or αMDG was incubated with SMIT or SGLT1 cRNA-injected oocytes and the sugar-induced steady-state current was measured at different membrane potentials (Fig. 4). In a SMIT cRNA-injected oocyte, the αMDG-induced current was about 30% of the *myo*-inositol-induced current at each voltage and the current

Table 2. Sugar transport by cRNA-injected oocytes

Solution injected	Na^+-dependent uptake (fmol/oocyte · hr)	
	myo-inositol	glucose
SMIT-cRNA	4,740 ± 370	85 ± 31
SGLT1-cRNA	359 ± 25	66,700 ± 6,300
H_2O	60 ± 32	26 ± 20

All values are the mean ± SEM (n = 6–7 oocytes). The total sugar concentration for both assays was 10 μM.

for both sugars increased with hyperpolarization of the membrane. In a SGLT1 cRNA-injected oocyte, the *myo*-inositol-induced current was about 10% of the αMDG-induced current. In contrast with SMIT, the currents mediated by SGLT1 saturated for both sugar substrates. In complementary experiments, the ability of SGLT1 to transport *myo*-inositol and SMIT to transport glucose was confirmed by measuring the transport of radioactive substrates into cRNA-injected oocytes. The results from a representative experiment are presented in Table 2. The rate of 10 μM *myo*-inositol transport by SGLT1 was about 7.5% of that by SMIT; in contrast, the rate of 10 μM D-glucose transport by SMIT was about 0.1% of that by SGLT1. Thus, SMIT and SGLT1 are not equally adept at transporting the two substrates.

By varying the external αMDG concentration and measuring the sugar-induced steady-state current, the $K_{0.5}^{\alpha MDG}$ for SMIT as a function of voltage was determined. The $K_{0.5}^{\alpha MDG}$ was about 30 mM (33 ± 10 mM at −150 mV; 44 ± 20 mM at −50 mV) and was virtually independent of voltage (*data not shown*). This value was about three orders of magnitude greater than the $K_{0.5}^{MI}$ (50 μM). The estimated $I_{max}^{\alpha MDG}$ was very similar to I_{max}^{MI} and increased with hyperpolarization of the membrane (*data not shown*). In the case of SGLT1 cRNA-injected oocytes, the *myo*-inositol-induced current was far from saturation, even at an external *myo*-inositol concentration of 100 mM (*data not shown*). Fitting the data to Eq. (1) gives an estimated $K_{0.5}^{MI} \approx 500$ mM, a value which is nearly 1,000-fold greater than $K_{0.5}^{\alpha MDG}$ (200 μM, Parent et al., 1992*a*). The $K_{0.5}^{MI}$ for SGLT1 was independent of membrane potential (*data not shown*).

Finally, different substrates at a concentration of 50 mM were tested with either SMIT or SGLT1 cRNA-injected oocytes. Figure 5 presents the substrate-induced currents at −150 mV normalized to the *myo*-inositol-induced current for the SMIT cRNA-injected oocytes and to the αMDG-induced current for the SGLT1 cRNA-injected oocytes. For SMIT, by assuming that I_{max} for any sugar is equal to I_{max}^{MI} the substrates are divided into four groups: (1) *myo*-inositol and *scyllo*-inositol were the best substrates with currents $\approx I_{max}^{MI}$ and apparent $K_{0.5}$s < 50 mM ($K_{0.5}^{MI}$ = 53 μM at V_m = −150 mV). (2) L-Fucose and L-xylose produced currents ≈ 50% I_{max}^{MI} and thus have

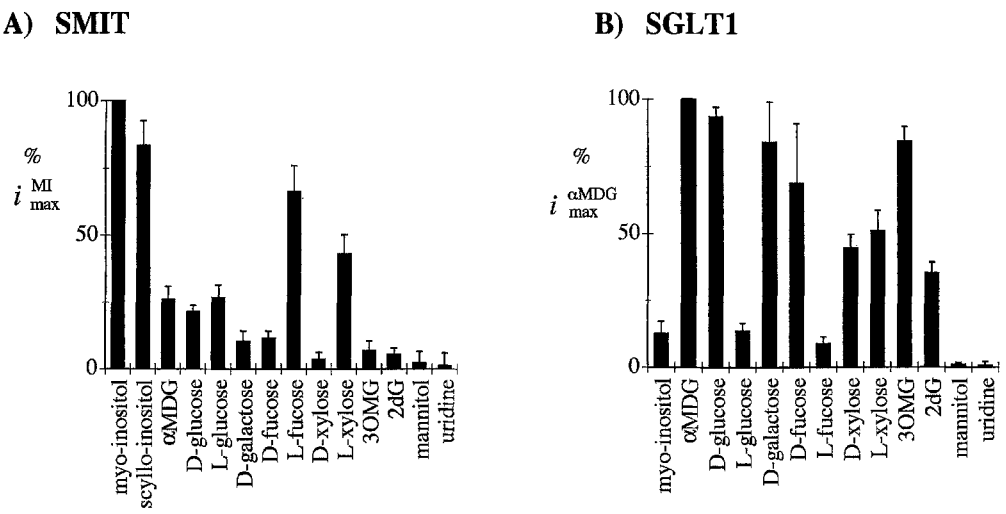

Fig. 5. Sugar specificity of SMIT and SGLT1. Oocytes were injected with either SMIT cRNA (*A*) or SGLT1 cRNA (*B*) and sugar-induced steady-state currents were measured at $V_m = -150$ mV with a sugar concentration of 50 mM. Data are the average of the current recorded from 3–7 oocytes, expressed as the percent of either the *myo*-inositol-induced current (*A*) or the αMDG-induced current (*B*). The average *myo*-inositol-induced current is −149 ± 21 nA ($n = 7$ oocytes) and the average αMDG-induced current is −2,155 ± 431 nA ($n = 5$ oocytes). (*30MG*) 3-*O*-methyl-D-glucose. (*2dG*) 2-deoxy-D-glucose.

apparent $K_{0.5} \approx 50$ mM. (3) αMDG, D-glucose, and L-glucose gave currents ≈ 25% I_{max}^{MI} yielding apparent $K_{0.5}$s > 50 mM. (4) Currents for D-galactose, D-fucose, D-xylose, 3-*O*-methyl-D-glucose, and 2-deoxy-D-glucose were < 10% I_{max}^{MI} and consequently apparent $K_{0.5} \gg 50$ mM. Of note, L-fucose and L-xylose are much better substrates than their D-stereoisomers. The ability of the different sugars to be transported by SMIT is not due to contamination by *myo*-inositol; most sugars exhibiting currents > 25% I_{max}^{MI} have negligible amounts of *myo*-inositol (< 0.002 mol %, Table 1), which at 50 mM sugar yields *myo*-inositol concentrations << $K_{0.5}^{MI}$. In a similar manner, the sugar substrates for SGLT1 are divided into three groups. The best substrates were αMDG, D-glucose, D-galactose, D-fucose, and 3-*O*-methyl-D-glucose, with currents ≈ $I_{max}^{\alpha MDG}$ and apparent $K_{0.5}$ < 50 mM ($K_{0.5}^{\alpha MDG}$ = 230 μM at $V_m = -150$ mV, Parent et al., 1992*a*). D-Xylose, L-xylose, and 2-deoxy-D-glucose were good substrates, giving currents ≈ 50% $I_{max}^{\alpha MDG}$ and apparent $K_{0.5} \approx 50$ mM. *Myo*-inositol, L-glucose, and L-fucose were poor substrates, producing currents < 15% $I_{max}^{\alpha MDG}$ and apparent $K_{0.5}$ > 50 mM. These results are in good agreement with previous measurements of the inhibition of [^{14}C]-αMDG transport into SGLT1 cRNA-injected oocytes by unlabeled sugars (Ikeda et al., 1989) and electrophysiological data (Birnir et al., 1991). In general, the D-sugars are better substrates than the L-sugars, with the exception of xylose where D and L isomers are transported with the same efficiency. In this case, the contamination of the different sugars with glucose is more problematical (Table 1); at 50 mM sugar the concentration of glucose is 100 and 150 μM for αMDG and D-fucose, respectively, values which are near the $K_{0.5}^{\alpha MDG}$. However, at least for αMDG, radioactive tracer and electrophysiological data at total sugar concentrations <1 mM clearly indicate that αMDG is an efficient substrate for SGLT1. In any event, with the exception of L-xylose, the various sugars can be used to clearly distinguish between SMIT and SGLT1: *myo*-inositol, *scyllo*-inositol, and L-fucose are the preferred substrates for SMIT and αMDG, D-glucose, D-galactose, D-fucose, and 3-*O*-methyl-D-glucose are excellent substrates for SGLT1. For both cotransporters, essentially no substrate-induced current was observed with mannitol and uridine; uridine is transported by the Na^+/nucleoside transporter (Pajor & Wright, 1992) which has a high degree of amino acid similarity with both SGLT1 and SMIT (61 and 47% identity, respectively). To summarize, the sugar selectivity for SMIT was *myo*-inositol, *scyllo*-inositol > L-fucose > L-xylose > αMDG, D-glucose, L-glucose > D-galactose, D-fucose, 3-*O*-methyl-D-glucose, 2-deoxy-D-glucose, D-xylose and for SGLT1 was αMDG, D-glucose, D-galactose, 3-*O*-methyl-D-glucose, D-fucose > L-xylose, D-xylose, 2-deoxy-D-glucose > *myo*-inositol, L-glucose, L-fucose.

Presteady-State Current in SMIT cRNA-injected Oocytes

As already mentioned, SMIT cRNA-injected oocytes exhibit a relaxation current (Fig. 1*A*). Such a presteady-state current was first observed and investigated for the Na^+/glucose cotransporter (Birnir et al., 1991; Parent et al., 1992*a*; Loo et al., 1993), and more recently for the Na^+/Cl^-/GABA cotransporter (Mager et al., 1993). Fig-

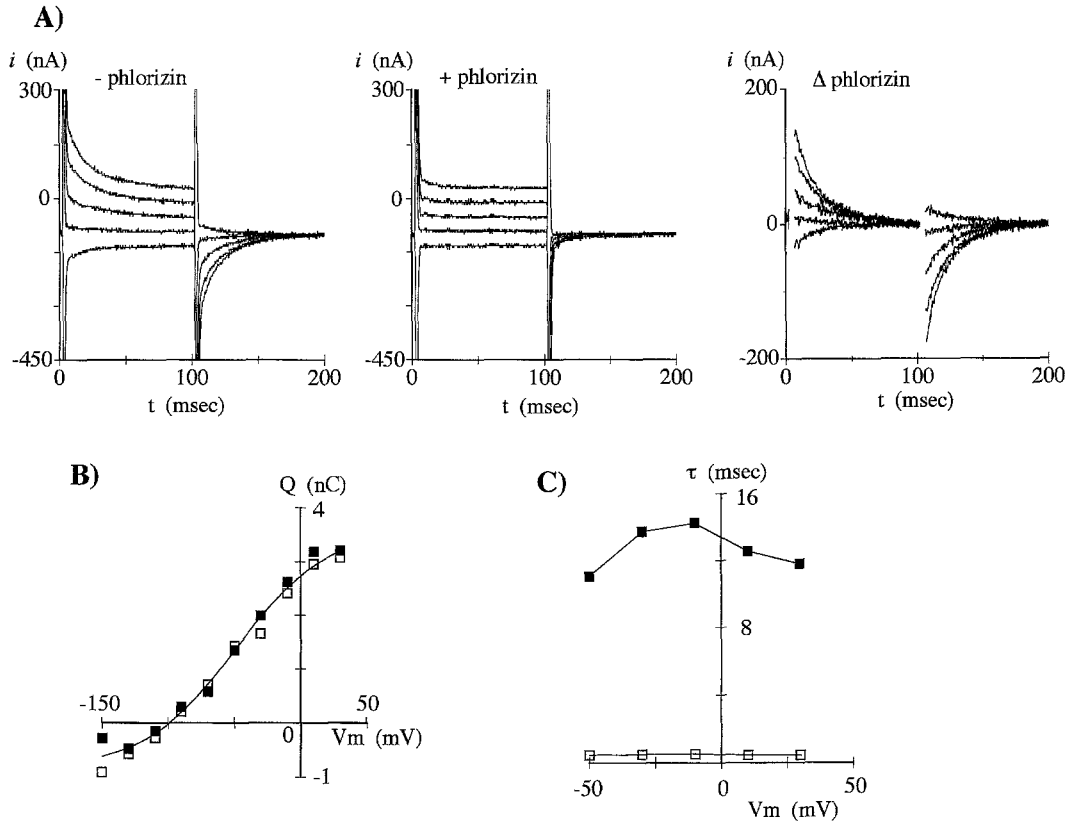

Fig. 6. Presteady-state current and charge movement in a SMIT cRNA-injected oocyte. (*A*) Measurement of the presteady-state current. On the left are the total current transients recorded from a SMIT cRNA-injected oocyte in the absence of external *myo*-inositol ($V_{hold} = -100$ mV). The addition of 0.5 mM phlorizin to the bath greatly reduced the presteady-state currents (middle panel). The phlorizin-sensitive presteady-state currents due to SMIT1 were obtained by subtraction of the total current transients recorded in the presence and absence of phlorizin (right panel). (*B*) Charge movement as a function of membrane potential. The charge Q was obtained by integration of the phlorizin-sensitive presteady-state currents. (□) and (■) denote the ON and OFF charge transfers, respectively. The curve drawn according to the Boltzmann relation:

$$Q(V_m) = Q_{hyp} + Q_{max}/[1 + \exp((V_t - V_{0.5})zF/RT)] \quad (5)$$

where $Q_{max} = (Q_{dep} - Q_{hyp})$. Q_{dep} is the limiting charge movement at large depolarizations, Q_{hyp} is the limiting charge movement at large hyperpolarizations, Q_{max} (4.3 nC) is the maximum charge transferred, V_m is the test pulse, $V_{0.5}$ (–49 mV) is the membrane voltage for $0.5Q_{max}$, z (–0.9) is the apparent valence of the movable charge, F is Faraday's constant, R is the gas constant, and T is the absolute temperature (*C*) Voltage dependence of the time constants τ_1 and τ_2. The total transient current relaxation (left panel of Fig. 6*A*) was fit by the sum of two exponential functions: the current attributable to SMIT (■) with a time constant τ_2 and the oocyte membrane capacitance (□) with a time constant τ_1. Identical results for τ_2 were obtained when the phlorizin-sensitive presteady-state currents (right panel of Fig. 6*A*) were fit to a single exponential function.

ure 6*A* illustrates the method for measuring the relaxation current. Current traces were recorded from a SMIT cRNA-injected oocyte bathed in a solution containing 100 mM Na and held at $V_{hold} = -100$ mV. Upon a step change in membrane voltage, the current rapidly increased and subsequently decayed over about 50 msec to a steady-state value. The initial fast transient ($\tau_1 \approx 0.5$ msec) is due to the oocyte membrane capacitance and was observed for both SMIT cRNA- and H_2O-injected oocytes. The slower transient ($\tau_2 \approx$ 10–14 msec) is not observed in H_2O-injected oocytes and is abolished by the addition of 0.5 mM phlorizin. Subtraction of the current recorded in the presence of phlorizin from that recorded in its absence gives the phlorizin-sensitive component of the presteady-state current, which represents the contribution of SMIT to the total presteady-state current. The phlorizin-sensitive presteady-state currents are identical for both the ON and OFF responses (the voltage jump from V_{hold} to V_m and the subsequent return from V_m to V_{hold}, respectively).

Integration of the area under the curves for the phlorizin-sensitive presteady-state currents yielded the charge movement (Q) for each test voltage pulse both in the ON- and OFF-directions (Fig. 6*B*). The charge movement of the ON response is virtually identical to that of the OFF response. At each test potential, the average of Q_{on} and Q_{off} was fit to the Boltzmann relation:

$$Q(V_m) = Q_{hyp} + (Q_{max}/[1 + \exp((V_m - V_{0.5})zF/RT)]) \quad (3)$$

where $Q_{max} = (Q_{dep} - Q_{hyp})$, Q_{dep} is the limiting charge movement at large depolarizations, Q_{hyp} is the limiting charge movement at large hyperpolarizations, V_m is the membrane potential of the test pulse, $V_{0.5}$ is the voltage for $0.5Q_{max}$, z is the apparent valence of the moving particle, F is Faraday's constant, R is the gas constant, and T is the absolute temperature. The values obtained for these parameters are: Q_{max} = 4.3 nC, z = –0.9, and $V_{0.5}$ = –49 mV.

The total current transients (Fig. 6*A*) were fit by the sum of two exponentials giving a fast time constant, τ_1, and a slow time constant, τ_2 (Fig. 6*C*). τ_1 was <1 msec over the voltage range 30 to –50 mV and was due to the capacitive transient of the oocyte membrane (*see* Loo et al., 1993). τ_2 varied from 10 to 14 msec over the same voltage range and represented the presteady-state current associated with SMIT. Similarly, the total current transients for SGLT1 cRNA-injected oocytes were dissected into two exponential components with a voltage-independent τ_1 and voltage-dependent τ_2 which varied from 12 to 19 msec between 50 and –30 mV (Panayotova-Heiermann, Loo & Wright, 1994).

In SGLT1 in the absence of sugar, phlorizin inhibited a component of the steady-state currents generated by the cotransporter (Umbach, Coady & Wright, 1990; Parent et al., 1992*b*). This Na^+ leak pathway constituted 5 to 15% of the sugar-induced currents. Phlorizin did not block the steady-state currents associated with SMIT in the absence of *myo*-inositol (Fig. 6*A*). This suggests that the Na^+ leak pathway is negligible or absent in SMIT. However, future experiments on oocytes with higher levels of expression (by an order of magnitude) are required to study this pathway.

Discussion

In view of the strong amino acid sequence similarity between SMIT and SGLT1 (49% identity) and the chemical similarity of their primary sugar substrates (D-glucose and *myo*-inositol), the above experiments were undertaken to measure the kinetics and substrate specificity of SMIT for comparison with those of SGLT1. Although SMIT and SGLT1 differ markedly with respect to preferred substrates (Fig. 5), there are many similarities in their kinetics of transport (Table 3). Each protein has a $K_{0.5}$ for the primary substrate ≤200 μM. SMIT and SGLT1 are capable of transporting both αMDG and *myo*-inositol; however, they discriminate by 1,000-fold between αMDG and *myo*-inositol as substrates. Phlorizin is an inhibitor of both transporters with an apparent K_I < 60 μM. Note that the phlorizin K_I for SMIT is 5- to 10-fold higher than that for SGLT1. Both SMIT and SGLT1 exhibit sigmoidal kinetics in response to increasing concentration of external Na^+. In each case, the Hill coefficient is approximately 2, suggesting that two Na^+ are transported per sugar molecule. No voltage dependence of the Hill coefficient was demonstrated by either protein. The estimated $K_{0.5}^{Na}$ for SMIT is two- to eight-fold higher than that for SGLT1. The *myo*-inositol-induced steady-state current of SMIT continuously increases over the voltage range of –10 to –150 mV (Fig. 1*D* and *E*); in contrast, the αMDG-induced steady-state current of SGLT1 saturates over the same voltage range (Fig. 4*B*; Fig. 2 of Parent et al., 1992*a*). Finally, in the presence of Na^+ and the absence of substrate and/or phlorizin, presteady-state currents are observed for both cotransporters. These transient currents apparently arise from the binding/dissociation of Na^+ and the reorientation of the cotransporter protein in the membrane in response to a change in the membrane's electric field (Loo et al., 1993). The magnitude of the steady-state and presteady-state currents and maximum charge transfer (Q_{max}) are appreciably lower for SMIT than SGLT1. Since the density of transporter estimated from charge transfer measurements agrees with estimates of transporter density from freeze-fracture studies of SGLT1 expressed in *Xenopus* oocytes (G.A. Zampighi, K.J. Boorer, M. Kremen, D.D.F. Loo and E.M. Wright, *submitted*), Q_{max} provides a measure of transporter density in the membrane. The difference in Q_{max} between SMIT and SGLT1 reflects lower expression of SMIT relative to SGLT1 in the oocyte membrane. Using $Q_{max} = C_T z_c e$, where e is the elementary charge, C_T is the density of transporters in the oocyte membrane and z_c is the apparent valence of the transporters (1), a density of 1×10^{10} SMIT molecules per oocyte is calculated, a value which is about 10% of that obtained for human SGLT1 (Loo et al., 1993).

Table 3. Comparison of SMIT and SGLT1 kinetic parameters

	$K_{0.5}^{\alpha MDG}$	$K_{0.5}^{MI}$	$K_I^{phlorizin}$	$K_{0.5}^{Na}$	Hill coefficient (*n*)
SGLT1	200 μM[b]	500 mM	6–10 μM[c]	35 mM[a,b]	1.9[b]
SMIT	50 mM	50 μM	55 μM[a]	75 mM[a]	1.8

[a] Indicates a voltage-sensitive parameter (value at V_m = –50 mV is shown). Sources: [b]Parent et al., 1992*a*. [c]Ikeda et al., 1989.

The similarities in the kinetics of SMIT and SGLT1 suggest that the two cotransporters share a common transport mechanism. Following the approach used previously for SGLT1 (Parent et al., 1992*b*), we propose a model for coupled Na^+ and *myo*-inositol transport by SMIT. We first propose a simple kinetic scheme (Fig. 7*A*), and then computer simulations are carried out until one set of rate constants account for the global kinetics observed for SMIT (Fig. 7*B*).

A six-state ordered model with mirror symmetry where external Na^+ binds first is assumed. Furthermore,

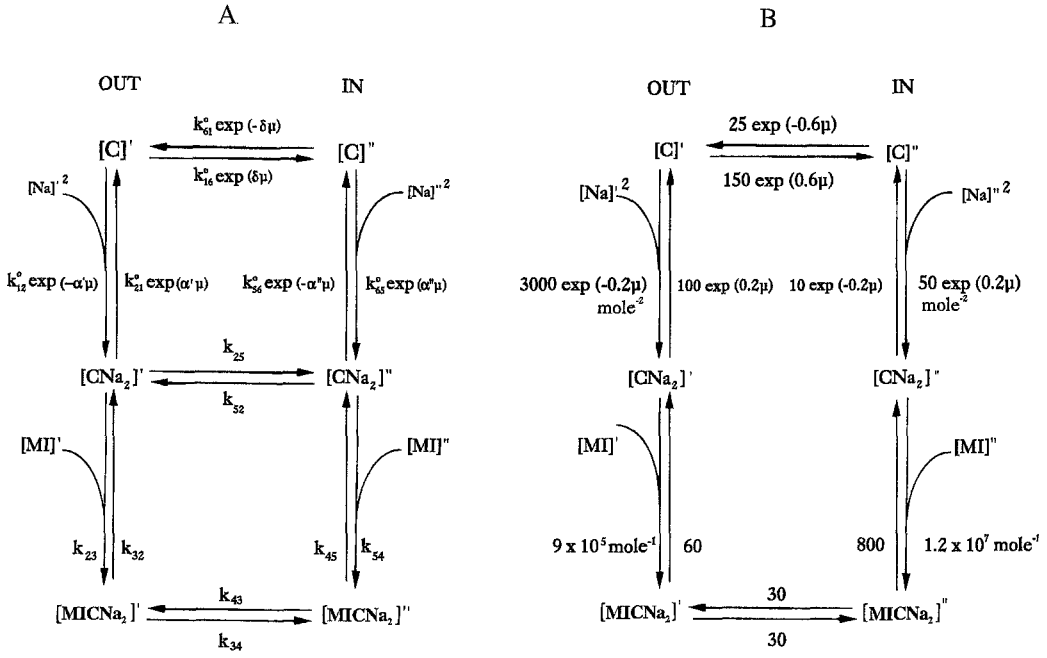

Fig. 7. Six-state kinetic model for Na^+/*myo*-inositol cotransport. (*A*) Transport is described as a six-state nonrapid equilibrium model where the unloaded protein has a valence of −2, and the ligand binding sites may face the outer or inner membrane/solution interfaces. To greatly simplify the model, Na^+ binding is described as a single reaction step. The voltage-dependent reactions are Na^+ binding and dissociation, and the state transition of the charged, unloaded protein ($C' \rightleftharpoons C''$). α and δ are phenomenological constants that describe the fraction of the membrane voltage sensed by the Na^+ binding and protein conformational steps. $\mu = FV/RT$. The formal description of the model, the assumptions and formulation of the steady-state and presteady-state current equations were presented previously (Parent et al., 1992*b*). (*B*) The rate constants of the kinetic model that account for SMIT kinetics (Fig. 8). The numerical values were determined by iterative numerical simulations, and the rate constants are in units of sec^{-1}, sec^{-1} mol^{-1}, or sec^{-1} mol^{-2}.

the protein is assumed to have two Na^+ binding sites, a valence of −2, and one *myo*-inositol binding site. State transitions include three transmembrane steps: one charge transport step ($C' \rightleftharpoons C''$), one ternary complex transition ($C'Na_2 \rightleftharpoons C''Na_2$) in the absence of substrate, and one transition of the fully loaded complex ($C'Na_2S \rightleftharpoons C''Na_2S$). There are additional individual steps for the binding of Na^+ and substrate at each surface. Current is carried by the unloaded protein ($C' \rightleftharpoons C''$), while the transitions of the partially and fully loaded protein ($C'Na_2 \rightleftharpoons C''Na_2$ and $C'Na_2S \rightleftharpoons C''Na_2S$, respectively) are electrically silent. Na^+ binding at each surface of the protein is voltage dependent. Voltage is assumed to affect the rates via two phenomenological constants α and δ: α' and α'' represent the fractional dielectric distance between the external and internal Na^+ binding sites and the membrane-solutions interfaces, and δ ($\alpha' + \delta + \alpha'' = 1$) represents the fractional dielectric distance over which the ion binding sites move. Each of the 14 reaction steps are assumed to be first order. Under zero-*trans* conditions, the steady-state current is $I = -2F\ (k_{16}[C]' - k_{61}[C]'')$ and the presteady-state current is: $I = -2F\{\alpha'(k_{12}[C]' - k_{21}[CNa_2]') + \delta(k_{16}[C]' - k_{61}[C]'') + \alpha''(k_{56}[CNa_2]'' - k_{65}[C]'')\}$. Analytical solutions for the steady-state distribution of the six protein states (C', $C'Na_2$, $C'Na_2S$, C'', $C''Na_2$, $C''Na_2S$) and numerical methods for the presteady-state behavior of such a model for SGLT1 have been described previously (Parent et al., 1992*b;* Loo et al., 1993).

A set of constants and coefficients have been obtained (Fig. 7*B*) that describe (Fig. 8) the steady-state SMIT *I-V* curves (Fig. 8*A*), the apparent *myo*-inositol and Na^+ affinities ($K_{0.5}^{MI}$ and $K_{0.5}^{Na}$) as a function of voltage (Figs. 8*B* and *C*), and the kinetics of SMIT presteady-state currents in the absence of *myo*-inositol—i.e., the charge movement (Fig. 8*E*) and the time course of the current relaxation (Fig. 8*D*). Further experiments are required to verify the model, such as testing the effect of external Na^+ on both steady-state and presteady-state kinetics, but to increase the sensitivity of the measurements it is necessary to increase the amount of expression about an order of magnitude, and to use the cut-oocyte preparation to obtain control over cytoplasmic ligand concentrations and increase the time resolution of the charge movement (Taglialatela et al., 1992; Loo, Bezanilla & Wright, 1994).

Nevertheless, comparison of SMIT kinetics with rabbit and human SGLT1 kinetics (Parent et al., 1992*b;* Loo et al., 1993) suggest remarkable similarities in the mechanism of *myo*-inositol and glucose cotransport. The

ordered six-state model accounts for the experimental observations, and the rate constants for the reaction steps are quite similar for the two proteins, e.g., the turnover numbers (5–25 sec^{-1}) and rate limiting steps (k_{61}) at 0 mV. The major differences are the apparent absence of a Na^+ leak pathway for SMIT, and the slower rate of external Na^+ binding to SMIT. The low rate of Na^+ binding accounts for the much lower apparent affinity for Na^+, $K_{0.5}^{Na}$ for SMIT is about an order of magnitude higher than SGLT1 at each membrane potential (more negative than −50 mV), and the difference in shape of the *I-V* curves. The D-glucose dependent currents through SGLT1 saturate at hyperpolarizing voltages (−100 to −150 mV), whereas the *myo*-inositol-dependent currents are supralinear over this voltage range. In terms of charge transfer, the Q_{max} for SMIT is about an order of magnitude lower than for rabbit and human SGLT1 (Loo et al., 1993; Panayotova-Heiermann et al., 1994; A. Hazama, D.D.F. Loo and E.M. Wright, *unpublished observations*), but the kinetic of charge transfer is similar for all three cotransporters. $V_{0.5}$, the voltage where $Q = 0.5Q_{max}$ is −50 mV for SMIT, −40 mV for human SGLT1, and +15 mV for rabbit SGLT1. The maximal value of the relaxation time constant for charge transfer is 14 msec at −20 mV for SMIT, 12 msec at −60 mV for human SGLT1, and 19 msec at +10 mV for rabbit SGLT1. Therefore, the kinetic rate constants for SMIT charge transfer closely approximate those for human SGLT1.

Altogether, this kinetic analysis, and the observations that phlorizin is an inhibitor and that *myo*-inositol, D-glucose, and L-xylose are substrates, albeit in some cases with low affinity, for both SMIT and SGLT1, strongly suggest that these two members of the same gene family share many structural features and transport mechanisms. It will be interesting to determine if other Na^+-dependent cotransporters in this family also share these properties.

With regards to sugar specificity, SMIT and SGLT1 display clear differences. SMIT greatly prefers *myo*-inositol and the nearly identical *scyllo*-inositol as substrates. In addition, L-fucose and L-xylose are good substrates; the L-enantiomers of these sugars are transported much more efficiently than the D-stereoisomers. For SGLT1, αMDG, D-glucose, and D-galactose are the best substrates; both D-fucose and 3-*O*-methyl-D-glucose are transported at about 70–80% of the rate of αMDG. With the exception of xylose, SGLT1 transports D-sugars much better than their L-counterparts. As previously mentioned, it is interesting that both SMIT and SGLT1 are capable of transporting either *myo*-inositol or αMDG, albeit with about 1,000-fold discrimination between the primary and secondary substrates (Table 3). Neither protein is capable of transporting uridine, a substrate for the Na^+/nucleoside transporter which shares significant amino acid similarity with SMIT and SGLT1.

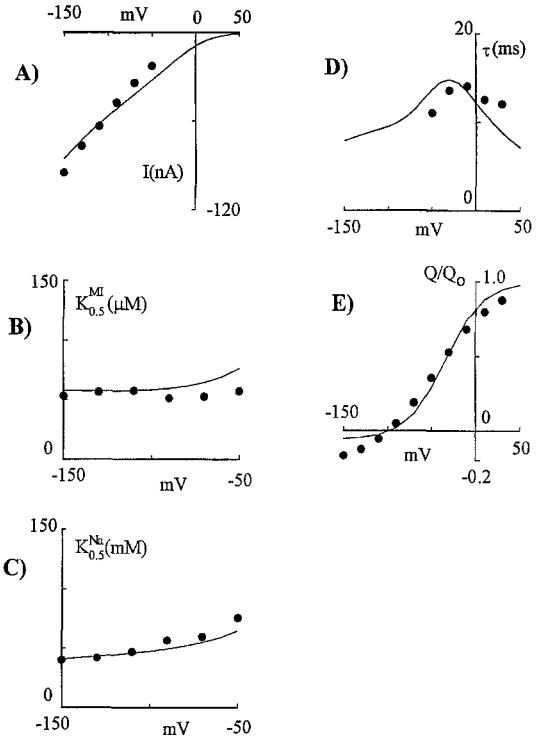

Fig. 8. Model prediction for SMIT using the rate constants and coefficients determined from numerical simulations (Fig. 7*B*). The total number of transporters in the oocyte membrane is 1.3×10^{10}, as indicated by Q_{max} measurements. The experimental data and simulations are shown under zero-*trans* conditions. (*A*) The steady-state *myo*-inositol-induced current as a function of voltage ($[MI]_o$ = 1 mM). (*B*) The $K_{0.5}^{MI}$ *vs.* voltage relationship at a fixed external Na^+ of 100 mM. (*C*) The $K_{0.5}^{Na}$ *vs.* voltage relationship at a fixed $[MI]_o$ of 500 μM. (*D*) The time constant τ for transient current relaxations at $[Na^+]_o$ = 100 mM and $[MI]_o$ = 0. The holding potential was −100 mV and the membrane voltage was rapidly stepped to a series of potentials between +50 and −150 mV (*see* Fig. 6*C*). (*E*) The charge transfer Q as a function of voltage. The transient currents seen in *D* are integrated for each voltage step between −150 and +50 mV and are plotted as a function of voltage. Q has been normalized by Q_o, the limiting charge transfer at the depolarizing limit. In all experiments the measured data (●) are described qualitatively by the model results (continuous lines). Numerical simulations were performed at the temperature of the experiments (25°C).

Na^+-dependent *myo*-inositol transport has been described in a wide variety of tissues, and the transport kinetics are very similar to those described here for SMIT (*see* Garcia-Perez & Burg, 1991). In addition to the transporter's role in osmoregulation of cells, there have been suggestions that the transporters are involved in the chronic complications of diabetes (*see* Del Monte et al., 1991; Yorek et al., 1991*b*). Acute exposure of cells to high D-glucose concentrations inhibits *myo*-inositol transport, and the sugar specificity of the effect, *myo*-inositol > L-fucose > L-xylose > D-xylose, L-glucose (Yorek et al., 1991*a*) is similar to the specificity of SMIT reported here. Since plasma levels of both L-fucose and

D-glucose increase in the serum of diabetic patients, this suggests that disturbances in *myo*-inositol metabolism in diabetes may be related to inhibition of *myo*-inositol transport.

Based on the clear differences in the sugar selectivity exhibited by SMIT and SGLT1, the construction of chimeric transporter molecules, part SMIT and part SGLT1, should permit the identification of amino acid residues involved in the discrimination between different sugar substrates.

We thank John Welborn for the HPLC analysis of the sugar substrates. This work was supported by grants from the National Institutes of Health DK19567, DK42479 and NS25554.

References

Birnir, B., Loo, D.D.F., Wright, E.M. 1991. Voltage-clamp studies of the Na^+/glucose cotransporter cloned from rabbit small intestine. *Pfluegers Arch.* **418:**79–85

Colman, A. 1984. Translation of eukaryotic messenger RNA in Xenopus oocytes. *In:* Transcription and Translation—A Practical Approach. B.D. Hames, and S.J. Higgins, editors. pp. 271–302. IRL, Oxford

Del Monte, M.A., Rabbani, R., Diaz, T.C., Lattimer, S.A., Nakamura, J., Brennan, M.C., Greene, S.A. 1991. Sorbitol, *myo*-inositol, and rod outer segment phagocytosis in cultured hRPE cells exposed to glucose: In vitro model of myo-inositol depletion hypothesis of diabetic complications. *Diabetes* **40:**1335–1345

Garcia-Perez, A., Burg, M.B. 1991. Renal medullary organic osmolytes. *Physiol. Rev.* **71:**1081–1115

Hediger, M.A., Coady, M.J., Ikeda, T.S., Wright, E.M. 1987. Expression cloning and cDNA sequencing of the Na^+/glucose cotransporter. *Nature* **330:**379–381

Ikeda, T.S., Hwang, E.S., Coady, M.J., Hirayama, B.A., Hediger, M.A., Wright, E.M. 1989. Characterization of a Na^+/glucose cotransporter cloned from rabbit small intestine. *J. Membrane Biol.* **110:**87–95

Krieg, P.A., Melton, D. 1984. Functional messenger RNAs are produced by SP6 *in vitro* transcription of cloned CDNAs. *Nucleic Acids Res.* **12:**7057–7070

Kwon, H.M., Yamauchi, A., Uchida, S., Preston, A.S., Garcia-Perez, A., Burg, M.B., Handler, J.S. 1992. Cloning of the cDNA for a Na^+/*myo*-inositol cotransporter, a hypertonicity stress protein. *J. Biol. Chem.* **267:**6297–6301

LaCourse, W.R., Mead, D.A., Johnson, D.C. 1990. Anion-exchange separation of carbohydrates with pulsed amperometric detection using a pH-selective reference electrode. *Anal. Chem.* **62:**220–224

Loo, D.D.F., Bezanilla, F., Wright, E.M. 1994. Two voltage-dependent steps are involved in the partial reactions of the Na^+/glucose cotransporter. *FASEB J.* **8:**A1992

Loo, D.D.F., Hazama, A., Supplisson, S., Turk, E., Wright, E.M. 1993. Relaxation kinetics of the Na^+/glucose cotransporter. *Proc. Natl. Acad. Sci. USA* **90:**5767–5771

Mager, S., Naeve, J., Quick, M., Labarca, C., Davidson, N., Lester, H.A. 1993. Steady states, charge movements, and rates for a cloned GABA transporter expressed in *Xenopus* oocytes. *Neuron* **10:**177–188

Moper, K., Schultz, C.A., Chevolot, L., Germain, C., Revuelta, R., Dawson, R. 1992. Determination of sugars in unconcentrated seawater and other natural waters by liquid chromatography and pulsed amperometric detection. *Environ. Sci. Technol.* **26:**133–138

Pajor, A.M., Wright, E.M. 1992. Cloning and functional expression of a mammalian Na^+/nucleoside cotransporter. *J. Biol. Chem.* **267:**3557–3560

Panayotova-Heiermann, M., Loo, D.D.F., Wright, E.M. 1994. Sodium/D-Glucose cotransporter charge movements involve polar residues. *J. Biol. Chem.* **269:**21016–21020

Parent, L., Supplisson, S., Loo, D.D.F., Wright, E.M. 1992*a*. Electrogenic properties of the cloned Na^+/glucose cotransporter: I. Voltage-clamp studies. *J. Membrane Biol.* **125:**49–62

Parent, L., Supplisson, S., Loo, D.D.F., Wright, E.M. 1992*b*. Electrogenic properties of the cloned Na^+/glucose cotransporter: II. A transport model under nonrapid equilibrium conditions. *J. Membrane Biol.* **125:**63–79

Taglialatela, M., Toro, L., Stefani, E. 1992. Novel voltage clamp to record small, fast currents from ion channels expressed in *Xenopus* oocytes. *Biophys. J.* **61:**78–82

Umbach, J., Coady, M.J., Wright, E.M. 1990. Intestinal Na^+/glucose cotransporter expressed in Xenopus oocytes is electrogenic. *Biophys. J.* **57:**1218–1224

Yorek, M.A., Stefani, M.R., Dunlap, J.A., Ro, K.S., Davidson, E.P. 1991. Trans-hydroxyl group configuration on carbons 2 and 3 of glucose. *Diabetes* **40:**1016–1023

Yorek, M., Stefani, M.R., Moore, S.A. 1991. Acute and chronic exposure of mouse cerebral microvessel endothelial cells to increased concentrations of glucose and galactose: effect on myo-inositol metabolism, PGE2 synthesis, and Na^+/K^+-ATPase transport activity. *Metabolism* **40:**347–358